POU2F1 promotes hypertensive cardiac fibrosis by regulating mitochondrial homeostasis through PINK1/Parkin-dependent mitophagy

YONGBO MA*, XIAOZHE CHEN*, ZIXIAN LIU*, YULONG MA, CHUNLEI HOU, YUNFENG LI, MINGTAI GUI, BO LU, DEYU FU and MINGZHU WANG

Department of Cardiology, Yueyang Hospital of Integrated Traditional Chinese and Western Medicine, Shanghai University of Traditional Chinese Medicine, Shanghai 200437, P.R. China

Received December 3, 2025; Accepted July 23, 2026

DOI: 10.3892/mmr.2026.14001

Abstract. Hypertension-induced cardiac fibrosis is a major risk factor for heart failure; although disrupted mitochondrial homeostasis has been confirmed to serve a critical role in the pathological process, its upstream regulatory factors remain incompletely understood. In the current study, RNA sequencing and bioinformatics analyses identified POU domain class 2 transcription factor 1 (POU2F1) as a hub transcriptional regulator in the fibrotic cardiac tissues of spontaneously hypertensive rats (SHRs). The expression levels of POU2F1 were associated with the severity of myocardial fibrosis, and cardiac expression of PTEN-induced kinase 1 (PINK1) and Parkin in SHRs. Complementing these *in vivo* observations, angiotensin II stimulation significantly upregulated POU2F1 expression in cardiac fibroblasts (CFs) *in vitro*. Furthermore, POU2F1 expression exhibited a positive correlation with fibroblast activation, as indicated by α-smooth muscle actin fluorescence intensity. Mechanistically, POU2F1 knockdown attenuated CF activation, improved mitochondrial structure and energy metabolism, and restored PINK1/Parkin-mediated mitophagy balance *in vivo* and *in vitro*. Conversely, POU2F1 overexpression was associated with enhanced PINK1/Parkin-mediated mitophagy signaling. Crucially, through chromatin immunoprecipitation-quantitative PCR, electrophoretic mobility shift assay and dual-luciferase reporter assay, it was demonstrated that POU2F1 can directly bind to the PINK1 promoter to activate its transcription. In conclusion, the present study identified a novel role for POU2F1 in hypertensive cardiac fibrosis, demonstrating that it exacerbates disease progression by disrupting mitochondrial homeostasis through transcriptional activation of PINK1, accompanied by alterations consistent with enhanced PINK1/Parkin-mediated mitophagy.

Correspondence to: Dr Mingzhu Wang or Dr Deyu Fu, Department of Cardiology, Yueyang Hospital of Integrated Traditional Chinese and Western Medicine, Shanghai University of Traditional Chinese Medicine, 110 Ganhe Road, Shanghai 200437, P.R. China
E-mail: wangmingzhu@shutcm.edu.cn
E-mail: fdy65@126.com

*Contributed equally

Key words: hypertension, cardiac fibrosis, POU2F1, PINK1, mitophagy

Introduction

Hypertension is a notable global public health challenge, which affects >1 billion individuals worldwide, and remains a predominant contributor to cardiovascular morbidity and mortality (1). The chronic pressure overload induced by hypertension initiates a pathological cascade that drives cardiac fibrosis, ultimately culminating in serious adverse outcomes such as heart failure. This pathological process is characterized by the differentiation of cardiac fibroblasts (CFs) into myofibroblasts, marked by the emergence of α-smooth muscle actin (α-SMA) expression (2) and the excessive deposition of extracellular matrix (ECM) proteins, including collagen I and fibronectin (3). Notably, targeting this fibrogenic cascade has considerable therapeutic potential for preserving cardiac function and improving survival in patients with cardiovascular disease (4).

Mitochondrial homeostasis, which is defined as the dynamic equilibrium of mitochondrial function, morphology and mass, has increasingly been recognized as a key determinant underlying fibrotic progression (5-7). Mitophagy serves as a pivotal mechanism in orchestrating mitochondrial homeostasis. Mitophagy is a selective form of autophagy responsible for clearing damaged mitochondria, fine-tuning mitochondrial quality control largely through the canonical PTEN-induced kinase 1 (PINK1)/Parkin-mediated pathway (8-10). This pathway has been extensively documented to exert cardioprotective effects in pathological contexts, such as myocardial ischemia-reperfusion injury and cardiac hypertrophy (11-13). However, under sustained pathological stimuli, such as hypertension-induced pressure overload, mitophagy overactivation disrupts cardiac mitochondrial homeostasis by depleting functional mitochondria, triggering a bioenergetic crisis and thus exacerbating the progression of cardiovascular

diseases (14-17). The precise regulatory mechanism of excessive mitophagy has not yet been fully elucidated.

Transcriptional regulation represents a central control layer in numerous biological processes, which notably contributes to the pathogenesis of cardiovascular diseases. POU domain class 2 transcription factor 1 (POU2F1) has been implicated in both oncogenesis and cardiovascular pathologies (18,19), where it facilitates disease progression through modulation of angiotensin II (Ang II) signaling, AMPK activation and stress-responsive genes, including sestrin 2 (20,21). A recent study revealed that exercise training alleviates Ang II-induced activation of CFs by reducing POU2F1 expression (22). However, whether POU2F1 regulates mitophagy, particularly through the PINK1/Parkin pathway, in hypertensive cardiac fibrosis remains to be elucidated.

In the present study, RNA sequencing was performed to identify candidate transcription factors associated with hypertensive cardiac fibrosis. The present study aimed to investigate the functional role of POU2F1 in cardiac fibrotic remodeling and elucidate the molecular mechanisms underlying its regulation of mitochondrial homeostasis, with emphasis on the PINK1/Parkin-dependent mitophagy pathway.

Materials and methods

Animals. Male SHRs and male Wistar-Kyoto (WKY) rats (age, 5 weeks; weight, ~120 g) were purchased from Beijing Vital River Laboratory Animal Technology Co., Ltd. A total of 18 SHRs and 9 WKY rats were used in the current study. The rats were randomly divided into the following groups: WKY rats served as the normotensive control group (n=9). SHRs were randomly assigned to three groups: Untreated SHR group (n=10), SHR + AAV9-shNC group (n=4), and SHR + AAV9-shPOU2F1 (n=4). SHRs in the latter two groups received tail vein injections of AAV9-shNC or AAV9-shPOU2F1, respectively, at 14 weeks of age and were maintained for an additional 4 weeks before subsequent analyses. All rats were acclimated and maintained in the laboratory until 14 weeks of age, at which time SHRs had developed established hypertension and myocardial fibrosis and were subsequently subjected to further analyses. Hypertension was confirmed by measuring systolic blood pressure (SBP) using the tail-cuff method, and rats with SBP consistently >150 mmHg were considered hypertensive. Myocardial fibrosis was verified by Masson's trichrome staining and fibrosis-related protein expression analyses (23,24). The rats were housed under controlled temperature (22±2˚C) and relative humidity (50-60%) with a 12-h light/dark cycle. Animals were monitored daily for health and behavior throughout the study, with free access to food and water. Humane endpoints included severe weight loss (>20%), inability to access food or water, persistent lethargy or signs of severe distress; no animals reached these humane endpoints and no unexpected deaths occurred. All procedures were approved by the Animal Care and Use Committee of Yueyang Hospital of Integrated Traditional Chinese and Western Medicine (approval no. YYLAC-2023-182-1; Shanghai, China) and were conducted following the National Institutes of Health Guide for the Care and Use of Laboratory Animals (25). At 18 weeks of age, rats were anesthetized with inhaled isoflurane (3% for induction and 1.5-2% for maintenance in oxygen), administered via a nose cone, and subjected to echocardiographic examination. Euthanasia was performed using an overdose of inhaled isoflurane (5% in oxygen) for 10 min until complete respiratory arrest occurred. Death was confirmed by the cessation of spontaneous respiration, absence of heartbeat and loss of corneal reflex.

Cell culture. CFs were prepared from neonatal rats and cultured as described previously (26). Primary cardiac fibroblasts were isolated from the ventricles of 36 neonatal Sprague-Dawley rats (age, 1 day) obtained from Beijing Vital River Laboratory Animal Technology Co., Ltd. The neonatal rats were euthanized by decapitation prior to heart collection. Subsequently, the ventricles were isolated from the hearts, minced into small pieces in ice-cold Hank's balanced salt solution, and subjected to repeated enzymatic digestion with collagenase type II (cat. no. 17101-015; both Gibco, Thermo Fisher Scientific, Inc.) at 37˚C. The cells were then resuspended, plated in 10-cm dishes with Dulbecco's Modified Eagle Medium (cat. no. SH30243.01B; HyClone; Cytiva) supplemented with 10% fetal bovine serum (cat. no. 16000-044; Gibco; Thermo Fisher Scientific, Inc.) and cultured at 37˚C in 5% CO_2. After a 24-h incubation, the cells were washed with phosphate-buffered saline (PBS) to remove cellular debris and non-adherent cells. Cell cultures yielded by this procedure were used as CFs based on their typical spindle-shaped morphology and adherence characteristics. Ang II (cat. no. HY-13948; MedChemExpress) was dissolved in sterile ultrapure water (cat. no. ST872; Beyotime Biotechnology) to prepare the stock solution. Cells treated with the corresponding volume of sterile ultrapure water were used as the vehicle control. Primary CFs were treated with Ang II at a concentration of 1 μmol/l for 48 h at 37˚C, whereas control cells were maintained in serum-supplemented medium.

Echocardiography. Cardiac function was evaluated using echocardiography (27,28). Rats were anesthetized with inhaled isoflurane (3% for induction and 1.5-2% for maintenance in oxygen), which was administered via a nose cone, and were then positioned in a supine position on a heated platform. Echocardiographic M-mode images were obtained from a parasternal short axis view at the level of the papillary muscles. A Vevo 2100 instrument (VisualSonics, Inc.) equipped with an MS-400 imaging transducer was used to measure interventricular septal diastolic thickness (IVSD), interventricular septal systolic thickness (IVSS), left ventricular end-diastolic diameter (LVIDD), LV end-systolic diameter (LVIDS), left ventricular posterior wall diastolic thickness (LVPWD) and left ventricular posterior wall systolic thickness (LVPWS).

Histopathological examination. Cardiac tissues were removed, rinsed with PBS, fixed in 4% paraformaldehyde at 4˚C for 24 h, dehydrated with graded ethanol, embedded in paraffin and cut into 5-μm sections. The heart sections were subsequently processed for Masson trichrome staining to evaluate myocardial fibrosis as previously described (29,30). For immunohistochemical staining, the sections were deparaffinized, rehydrated and subjected to microwave-assisted antigen retrieval in citrate buffer (pH 6.0) at 100˚C for 20 min, followed by three washes with PBS. After blocking with

5% BSA (cat. no. ST023; Beyotime Biotechnology) at room temperature for 1 h, the sections were incubated with primary antibodies against POU2F1 (cat. no. 10387-1-AP; 1:1,000; Proteintech Group, Inc.), collagen I (cat. no. 14695-1-AP; 1:500; Proteintech Group, Inc.) and α-SMA (cat. no. ab7817; 1:1,000; Abcam) overnight at 4˚C, followed by incubation with horseradish peroxidase-conjugated goat anti-rabbit (cat. no. A0208; 1:1,000; Beyotime Biotechnology) and anti-mouse IgG (cat. no. A0216; 1:1,000; Beyotime Biotechnology) at room temperature for 1 h. Immunoreactive signals were visualized using 3DAB), followed by hematoxylin counterstaining. Images were captured using a light microscope, and fibrosis was quantified using ImageJ software (version 1.8.0; National Institutes of Health).

Transmission electron microscopy (TEM). Cardiac tissues (1 mm^3) were fixed in 2.5% glutaraldehyde at 4˚C for 24 h, washed with PBS and post-fixed with 1% osmium tetroxide at 4˚C for 2 h. Dehydration was carried out through sequential immersion in 30, 50, 70 and 80% ethanol solutions, followed by a 1:1 mixture of 90% ethanol and 90% acetone. The samples were embedded in epoxy resin at 60˚C for 48 h. Ultrathin sections (50 nm) were stained with 2% uranyl acetate for 15 min at room temperature and 2% lead citrate for 10 min at room temperature, then examined under a transmission electron microscope (Tecnai G2 Spirit BioTWIN; Thermo Fisher Scientific, Inc.) (31,32).

RNA-seq. Total RNA was extracted from cardiac tissues using TRIzol® reagent (Invitrogen; Thermo Fisher Scientific, Inc.). RNA concentration was measured with a NanoDrop ND-2000 spectrophotometer (NanoDrop; Thermo Fisher Scientific, Inc.) and RNA integrity (RNA integrity number ≥7) was assessed using an Agilent 2100 Bioanalyzer (Agilent Technologies, Inc.). Library preparation and 150-bp paired-end sequencing were performed on an Illumina NovaSeq 6000 platform (Illumina, Inc.) by Majorbio BioPharm Technology Co., Ltd. (33). Raw reads were quality-controlled using fastp (v0.23.2, github.com/OpenGene/fastp), and differentially expressed genes (DEGs) between the SHR and WKY groups were identified using DESeq2 (v1.38.3, bioconductor.org) with thresholds of $|\log_2(\text{fold change})|>1$ and adjusted $P\leq0.05$. Hierarchical cluster analysis of DEGs was performed using the OECloud tools (v1.26, cloud.oebiotech.com) to demonstrate the expression pattern of genes in different groups and samples. The transcription factor data of rats was obtained from AnimalTFDB v4.0 (https://guolab.wchscu.cn/AnimalTFDB4//#/).

Adeno-associated virus serotype 9 (AAV9) injection. To determine the role of POU2F1 in PINK1-mediated mitophagy and myocardial fibrosis *in vivo*, short hairpin RNA (shRNA) targeting POU2F1 (5'-TGCACAGGATCTTCAACAATT-3') or a negative control (NC) sequence (shNC, 5'-TTCTCC GAACGTGTCACGT-3') were cloned into AAV9 vectors and packaged into recombinant AAV9 particles, generating AAV9-shPOU2F1 and AAV9-shNC, respectively. The shRNA and the recombinant AAV9 vectors were constructed and packaged by Shanghai GenePharma Co., Ltd. SHRs were injected via the tail vein at 14 weeks of age with $2x10^{11}$ viral genomes/rat AAV9-shPOU2F1 or AAV9-shNC (in 200 μl PBS). Both groups were fed a standard diet and echocardiographic assessments were performed at 18 weeks of age. Subsequently, the rats were euthanized using an overdose of inhaled isoflurane as aforementioned.

Immunofluorescence staining. The CFs were fixed with 4% paraformaldehyde for 15 min, permeabilized with Triton X-100 for 10 min and blocked with 1% BSA (cat. no. ST023; Beyotime Biotechnology) for 1 h, all at room temperature. Subsequently, the cells were incubated overnight at 4˚C with a primary antibody against α-SMA (cat. no. ab7817; 1:100; Abcam). Alexa Fluor® 488-conjugated goat anti-mouse IgG (cat. no. A0428; Beyotime Biotechnology) was then applied at room temperature for 1 h, followed by DAPI (cat. no. C1002; Beyotime Biotechnology) counterstaining at room temperature for 5 min. Fluorescent images were captured using a fluorescence microscope (ECLIPSE Ni; Nikon Corporation).

MitoSOX and EdU staining. To measure mitochondrial superoxide levels, the CFs were incubated with MitoSOX Red (cat. no. M36008; Thermo Fisher Scientific, Inc.) for 10 min at 37˚C in the dark, according to the manufacturer's instructions. DAPI was used to stain the nuclei at room temperature for 10 min. Red fluorescence reflecting mitochondrial superoxide levels was captured using a confocal laser scanning microscope. For proliferation analysis, EdU incorporation was performed using the EdU kit (cat. no. C0071L; Beyotime Biotechnology) according to the manufacturer's protocol. Hoechst 33342 was used to stain the nuclei at room temperature for 10 min. ImageJ software (version 1.8.0) was employed to quantify MitoSOX fluorescence intensity and count the number of EdU-positive cells.

Gene overexpression and knockdown. For gene overexpression, the coding sequence of rat POU2F1 was cloned into the pcDNA3.1(+) vector (General Biol,). The CFs were then transfected with the POU2F1 plasmid or an empty vector control. For gene knockdown, shRNA constructs targeting POU2F1 or PINK1, and a NC, were purchased from Shanghai GenePharma Co., Ltd.; the selected sequences are listed in Table SI. CFs were seeded at a density of $2x10^5$ cells/well in 6-well plates and transfected 24 h after seeding. Transfection was performed using Lipofectamine® 2000 (Invitrogen; Thermo Fisher Scientific, Inc.) according to the manufacturer's instructions (34). Specifically, 2.5 μg plasmid DNA and 6 μl Lipofectamine 2000 reagent were incubated at 37˚C. The culture medium was replaced with fresh medium at 6 h, and the cells were cultured for 48 h after transfection before being harvested for subsequent experiments. CFs were co-transfected with oe-POU2F1 and sh-PINK1 plasmids simultaneously.

Dual-luciferase reporter gene assay. First, the rat PINK1 promoter sequence (-2,000 bp) was obtained from the National Center for Biotechnology Information (NCBI; ncbi.nlm.nih.gov/gene/), and the POU2F1 binding motif was predicted using Jaspar (jaspar.genereg.net/). The predicted POU2F1-binding sequence was identified as 5'-TATTTA AAT-3' (wild-type). A mutant sequence (5'-ATAAAGGGA-3') was generated by replacing the predicted POU2F1-binding motif. Both sequences were synthesized and cloned into the

pGL3-Basic luciferase reporter vector (Promega Corporation). Subsequently, the synthesized plasmids were subjected to Sanger sequencing to confirm the accuracy of the inserted sequences. The plasmids were then extracted using a plasmid extraction kit (Beijing Solarbio Science & Technology Co., Ltd.). 293T cells were co-transfected with WT or MUT PINK1 promoter reporter plasmids together with either the POU2F1 overexpression plasmid (pcDNA3.1-POU2F1, General Biol, Anhui, China) or the corresponding empty vector control (pcDNA3.1, both General Biol, Anhui, China). A total of 4 μg of plasmids was transfected into cells in each group using Lipofectamine 3000 (cat. no. L3000001; Invitrogen; Thermo Fisher Scientific, Inc.). After 6 h of incubation, the transfection medium was replaced with complete medium. At 48 h after transfection, cells were lysed, and firefly and Renilla luciferase activities were determined using the Dual-Luciferase Reporter Assay System (Promega Corporation). Firefly luciferase activity was normalized to Renilla luciferase activity, and relative promoter activity was calculated as the firefly/*Renilla* luciferase ratio (35).

Electrophoretic mobility shift assay (EMSA). EMSA was performed using the Chemiluminescent EMSA Kit (cat. no. GS009; Beyotime Biotechnology) according to the manufacturer's instructions (36). The WT and MUT oligonucleotide probes were designed according to the predicted POU2F1-binding site in the PINK1 promoter and synthesized by Beyotime Biotechnology. For the EMSA binding reaction, 4 μg purified protein (Cat. no. P04804; Solarbio Biotechnology) was incubated with 1 pmol biotin-labeled probe in binding buffer for 20 min at room temperature. For competitive EMSA, 100 pmol unlabeled competitor probes were added to the reaction mixture 20 min prior to the addition of the biotin-labeled probe. In the mutation assay, mutated biotin-labeled probes were used in place of WT probe. The reaction mixtures were resolved on a 6% polyacrylamide gel and transferred to a nylon membrane. The DNA oligomers were then crosslinked to the membrane via UV irradiation, and the biotin-labeled probes were detected using a chemiluminescent imaging system.

Seahorse metabolic assays. According to the manufacturer's instructions, mitochondrial stress was assessed using the Agilent Seahorse XF Cell Mito Stress Test Kit (cat. no. 103015-100; (Agilent Technologies, Inc.) to measure the oxygen consumption rate (OCR) of the CFs. For *ex vivo* experiments, CFs isolated from SHR and WKY rat hearts, as well as CFs isolated from AAV9-shNC- or AAV9-shPOU2F1-treated SHR rats, were subjected to Seahorse analysis. For *in vitro* experiments, Ang II-induced CFs transfected with shPOU2F1 or shNC were used. Briefly, 16,000 cells/well were seeded in a 96-well XF Cell Culture Microplate (Agilent Technologies, Inc.). OCR was measured at three timepoints, in basal conditions and following the addition of oligomycin (1.0 μg/ml), carbonyl cyanide-4-trifluoromethoxy phenylhydrazone (1.0 μmol/l) and rotenone + antimycin A (both at 0.5 μmol/l). Data were analyzed using Seahorse XF software (version 2.6; Agilent Technologies, Inc.).

Western blotting. The protein expression was analyzed by western blotting as described previously (37), with GAPDH used as an endogenous control. After total protein was extracted from rat ventricular tissue and CFs using RIPA buffer (Beyotime Biotechnology) supplemented with protease inhibitors and quantified by BCA assay, protein samples (25 μg/lane) were separated by 10% SDS-PAGE and transferred onto polyvinylidene difluoride membranes. The membranes were blocked with 5% skimmed milk at room temperature for 1 h and incubated with primary antibodies at 4˚C overnight. The next day, the membranes were washed three times with TBS-0.1% Tween-20 wash buffer for 10 min each. The membranes were incubated with secondary antibodies for 1 h at room temperature. Membranes were washed with TBS-0.1% Tween-20 wash buffer. The following antibodies were used in western blotting: Collagen I (cat. no. 14695-1-AP; 1:1,000; Proteintech Group, Inc.), α-SMA (cat. no. ab7817; 1:1,000; Abcam), POU2F1 (cat. no. 10387-1-AP; 1:2,000; Proteintech Group, Inc.), PINK1 (cat. no. 23274-1-AP; 1:1,000; Proteintech Group, Inc.), Parkin (cat. no. 14060-1-AP; 1:1,000; Proteintech Group, Inc.), LC3B (cat. no. 14600-1-AP; 1:1,000; Proteintech Group, Inc.), P62 (cat. no. 18420-1-AP; 1:5,000; Proteintech Group, Inc.) and GAPDH (cat. no. 10494-1-AP; 1:5,000; Proteintech Group, Inc.) primary antibodies, horseradish peroxidase-conjugated goat anti-mouse IgG (cat. no. A0216; 1:1,000; Beyotime Biotechnology), and horseradish peroxidase-conjugated goat anti-rabbit IgG secondary antibody (cat. no. A0208; 1:1,000; Beyotime Biotechnology). Chemiluminescent detection was performed and images were captured using the Tanon 5200 system (Tanon Science and Technology Co., Ltd.). The gray values were measured and analyzed using ImageJ software (version 1.8.0; National Institutes of Health).

Reverse transcription-quantitative PCR (RT-qPCR). Total RNA was extracted from cardiac tissue and CFs using a Total RNA Extraction Reagent (Shanghai Yeasen Biotechnology Co., Ltd.). After DNase treatment, the RNA was reverse-transcribed into cDNA using a cDNA Synthesis Kit (Shanghai Yeasen Biotechnology Co., Ltd.) according to the manufacturer's instructions. qPCR was performed using SYBR Green Master Mix (Shanghai Yeasen Biotechnology Co., Ltd.). The thermocycling conditions were as follows: initial denaturation at 95˚C for 5 min, followed by 40 cycles of denaturation at 95˚C for 10 sec and annealing/extension at 60˚C for 30 sec. A melting curve analysis was performed to verify amplification specificity. GAPDH was used as an internal control for normalization, and relative mRNA expression levels were calculated using the $2^{-\Delta\Delta Cq}$ method (38). Primer sequences are listed in Table SII.

Chromatin immunoprecipitation (ChIP)-qPCR assay. CFs were cultured to 80-90% confluence. CFs were cross-linked with 1% paraformaldehyde at room temperature for 10 min, and the crosslinking reaction was quenched with glycine at room temperature for 5 min. The cells were then resuspended in ChIP Sonication Cell Lysis Buffer (cat. no. 81804; Cell Signaling Technology, Inc.) supplemented with Protease Inhibitor Cocktail (PIC) and incubated on ice. Subsequently, chromatin was fragmented by sonication on ice using a sonicator (power, 20% amplitude; pulse duration, 5 sec on/5 sec off; total duration, 10 min) to obtain DNA fragments of appropriate size. The fragmented chromatin was diluted in ChIP Buffer (cat. no. 14231; Cell Signaling Technology, Inc.)

containing PIC to prepare a 2% input sample. The remaining chromatin was diluted in ChIP Dilution Buffer containing PIC and incubated overnight at 4˚C with an anti-POU2F1 antibody (cat. no. ab178869) or normal rabbit IgG (both 5 μg; cat. no. ab313801) (both from Abcam) as a NC. qPCR was performed using SimpleChIP® Universal qPCR Master Mix (Cell Signaling Technology, Inc.) according to the manufacturer's instructions to quantify the enrichment of POU2F1-bound PINK1 promoter regions. Primer sequences are listed in Table SIII. Detailed experimental methods are included in the previously published literature (39,40).

Cell viability assay. Cell viability of primary CFs in response to Ang II was assessed using the CCK-8 assay kit (cat. no. C0037; Beyotime Biotechnology) according to the manufacturer's instructions (41). Primary CFs were seeded into 96-well plates at $1x10^4$ cells/well and incubated for 24 h. Subsequently, the cells were treated with different concentrations of Ang II for 48 h. Following treatment, 10 μl of CCK-8 reagent was added to each well, and the cells were incubated at 37˚C for 2 h. The optical density at 450 nm was measured using a microplate reader to evaluate cell viability.

Statistical analysis. Data are presented as the mean ± standard deviation of ≥3 independent experiments. Statistical analyses were performed using GraphPad Prism 9.0 software (Dotmatics). Statistical tests, including one-way analysis of variance followed by Tukey's post hoc test and unpaired two-tailed Student's t-test, were conducted to determine significant differences between sample means. Correlations between variables were analyzed using Spearman's rank correlation analysis. $P<0.05$ was considered to indicate a statistically significant difference.

Results

POU2F1 upregulation and mitochondrial damage in myocardial fibrosis of SHRs. A significant increase in cardiac fibrosis was observed in SHRs compared with in the WKY control rats. Masson trichrome staining of cardiac apical tissue revealed disrupted cardiac architecture in SHRs, which was characterized by extensive blue-stained areas indicating collagen deposition and fibrotic remodeling (Fig. S1A). Western blotting confirmed elevated expression of the fibrosis markers collagen I and α-SMA in SHRs (Fig. S1B). Consistently, immunohistochemical staining revealed markedly stronger immunoreactivity for collagen I and α-SMA in the left ventricular myocardium of SHRs than in that of WKY rats (Fig. S1C). To characterize molecular alterations associated with cardiac fibrosis in SHRs, RNA-seq was performed on cardiac tissues from SHRs and WKY rats. Bioinformatics analysis identified 476 DEGs between the groups. By comparing the DEGs with a rat transcription factor database, 18 differentially expressed transcription factors were identified (Fig. 1A). Hierarchical clustering demonstrated the expression patterns of these transcription factors: 17 were upregulated in SHRs, whereas one was downregulated (Fig. 1B). Among these transcription factors, POU2F1 exhibited the most significant differential expression; western blotting and RT-qPCR confirmed upregulation of POU2F1 at both the mRNA and protein levels in SHRs (Fig. 1C and D). This increase was further supported by immunohistochemical analysis, which demonstrated enhanced POU2F1 staining in the myocardial tissues of SHRs (Fig. 1E). Notably, it was further observed that the area of cardiac fibrosis was closely correlated with both the mRNA ($\varrho=0.7250$) and protein ($\varrho=0.9091$) expression levels of POU2F1 (Fig. S1D).

TEM demonstrated mitochondrial ultrastructural damage in the cardiac tissues of SHRs, characterized by cristae disorganization and an increased number of mitochondria with abnormal morphology, including swelling and disrupted cristae (Figs. 1F and S1E). In addition, mitochondrial respiratory function, as assessed by OCR, was significantly impaired in SHRs, with decreased basal respiration, maximal respiration and ATP production-associated respiration (Fig. 1G). Notably, the expression levels of the key mitophagy regulators PINK1 and Parkin were significantly increased in the hearts of SHRs (Fig. 1H), suggesting dysregulation of the PINK1/Parkin-associated mitophagy pathway during hypertensive fibrogenesis. Furthermore, a strong positive correlation was observed between PINK1 and POU2F1 expression ($r=0.9441$, $P<0.001$; Fig. 1I).

POU2F1 upregulation and mitochondrial damage in Ang II-induced CFs. Primary CFs were treated with Ang II (0-100 μmol/l) for 48 h and cell viability was assessed using the CCK-8 assay. The results showed that 1 μmol/l Ang II maintained relatively higher cell viability. Therefore, 1 μmol/l Ang II was selected for subsequent experiments (Fig. S2A). Notably, the concurrent increase in EdU positivity (Figs. 2A and S2B) and α-SMA expression (Figs. 2B and S2C) demonstrated that Ang II-induced CFs underwent both proliferation and phenotypic activation (myofibroblast differentiation). These coordinated cellular responses contribute to pathological ECM accumulation during myocardial fibrosis (42). This finding was corroborated by significantly elevated protein levels of both collagen I and α-SMA in Ang II-treated CFs (Fig. S2D). Consistent with the *in vivo* findings, Ang II-induced CFs exhibited elevated mRNA and protein levels of POU2F1 (Fig. 2C and D). Furthermore, POU2F1 protein levels were positively correlated with α-SMA fluorescence intensity ($r=0.8951$, $P<0.001$; Fig. 2E).

In addition to POU2F1 upregulation, mitochondrial reactive oxygen species were assessed using mitoSOX Red staining (Fig. 2F). In Ang II-induced CFs, robust red fluorescence signals indicative of mitochondrial superoxide accumulation were observed, demonstrating heightened mitochondrial oxidative stress (Figs. 2F and S2E). Consistently, western blotting revealed marked upregulation of PINK1 and Parkin, suggesting potential activation of the mitophagy pathway (Figs. 2G and S2F). Furthermore, correlation analysis revealed a strong positive correlation between POU2F1 and PINK1 protein expression ($r=0.8671$, $P<0.001$; Fig. 2H).

POU2F1 knockdown reduces PINK1-mediated mitophagy and mitochondrial dysfunction in Ang II-induced CFs. To investigate the role of POU2F1 in PINK1-mediated mitophagy and myocardial fibrosis *in vitro*, a plasmid-based shRNA vector was constructed to specifically knock down POU2F1 expression, and the knockdown efficiency was confirmed by RT-qPCR analysis in CFs (Fig. S3A). In

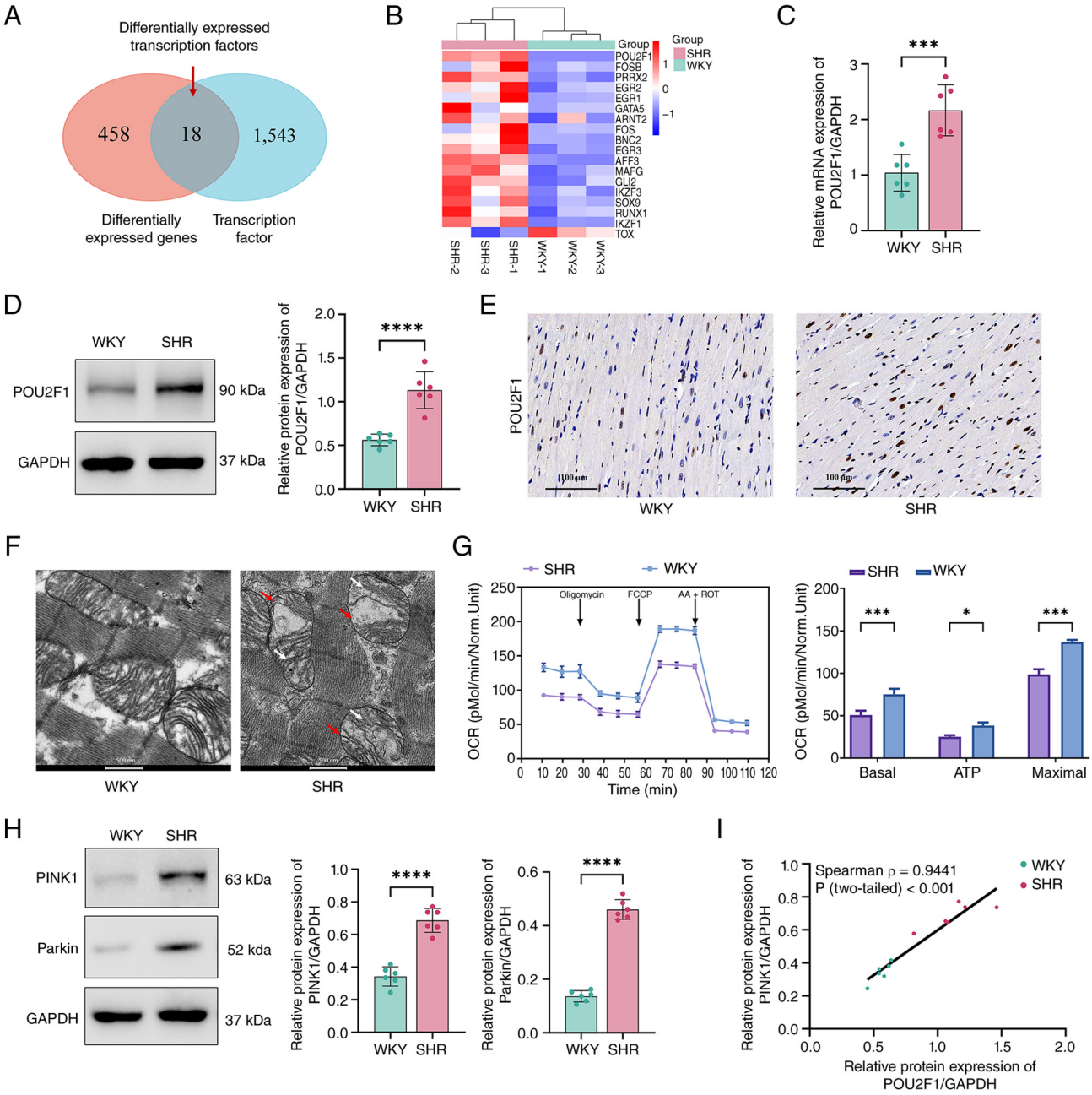

Figure 1. POU2F1 upregulation and mitochondrial damage in myocardial fibrosis of SHRs. (A) Overlap between transcription factors and differentially expressed genes in cardiac tissues of SHRs compared with WKY rats. (B) Heatmap representing the relative levels of differentially expressed transcription factors between WKY rats and SHRs. (C) mRNA levels of POU2F1 in cardiac tissues were detected by reverse transcription-quantitative PCR. (D) Protein levels of POU2F1 in cardiac tissues were detected by western blotting (n=6). (E) Representative immunohistochemical staining images of POU2F1 in left ventricular myocardial tissues from WKY rats and SHR. (scale bar, 100 μm). (F) Transmission electron microscopy was used to observe mitochondrial structure in cardiac tissue from WKY rats and SHRs (scale bar, 500 nm). White arrows indicate cristae disorganization; red arrows indicate damaged mitochondria. (G) Seahorse assay profile of OCRs in CFs following sequentially treatment with oligomycin, FCCP and AA + ROT. Quantitative analysis of mitochondrial function parameters (basal respiration, maximal respiration and ATP production) is shown in the bar charts (n=3). (H) Protein levels of PINK1 and Parkin in cardiac tissues were detected by western blotting (n=6). (I) Protein expression levels of PINK1 were positively correlated with POU2F1 expression (Spearman correlation, n=12). *P<0.05; ***P<0.001; ****P<0.0001. AA, antimycin A; FCCP, carbonyl cyanide-4-trifluoromethoxy phenylhydrazone; OCR, oxygen consumption rate; PINK1, PTEN-induced kinase 1; POU2F1, POU domain class 2 transcription factor 1; ROT, rotenone; SHR, spontaneously hypertensive rat; WKY, Wistar-Kyoto.

the shPOU2F1 group, mitoSOX levels were decreased, suggesting attenuated oxidative stress (Fig. 3A and C), and TEM further confirmed reduced mitochondrial ultrastructural damage (Fig. 3B and C). In addition, mitochondrial respiratory function was significantly increased upon POU2F1 knockdown (Fig. 3D). Concomitantly, under Ang II stimulation, the shPOU2F1 group showed a significant decrease in the expression levels of the mitophagy-related proteins PINK1, Parkin and LC3B, and an increase in P62 expression, indicating that silencing of POU2F1 inhibited the PINK1-mediated mitophagy pathway (Fig. 3E). Additionally, POU2F1 knockdown inhibited CF proliferation and α-SMA expression (Fig. 3F-H). Western blot analysis confirmed the decreased expression of collagen I and α-SMA in cells with

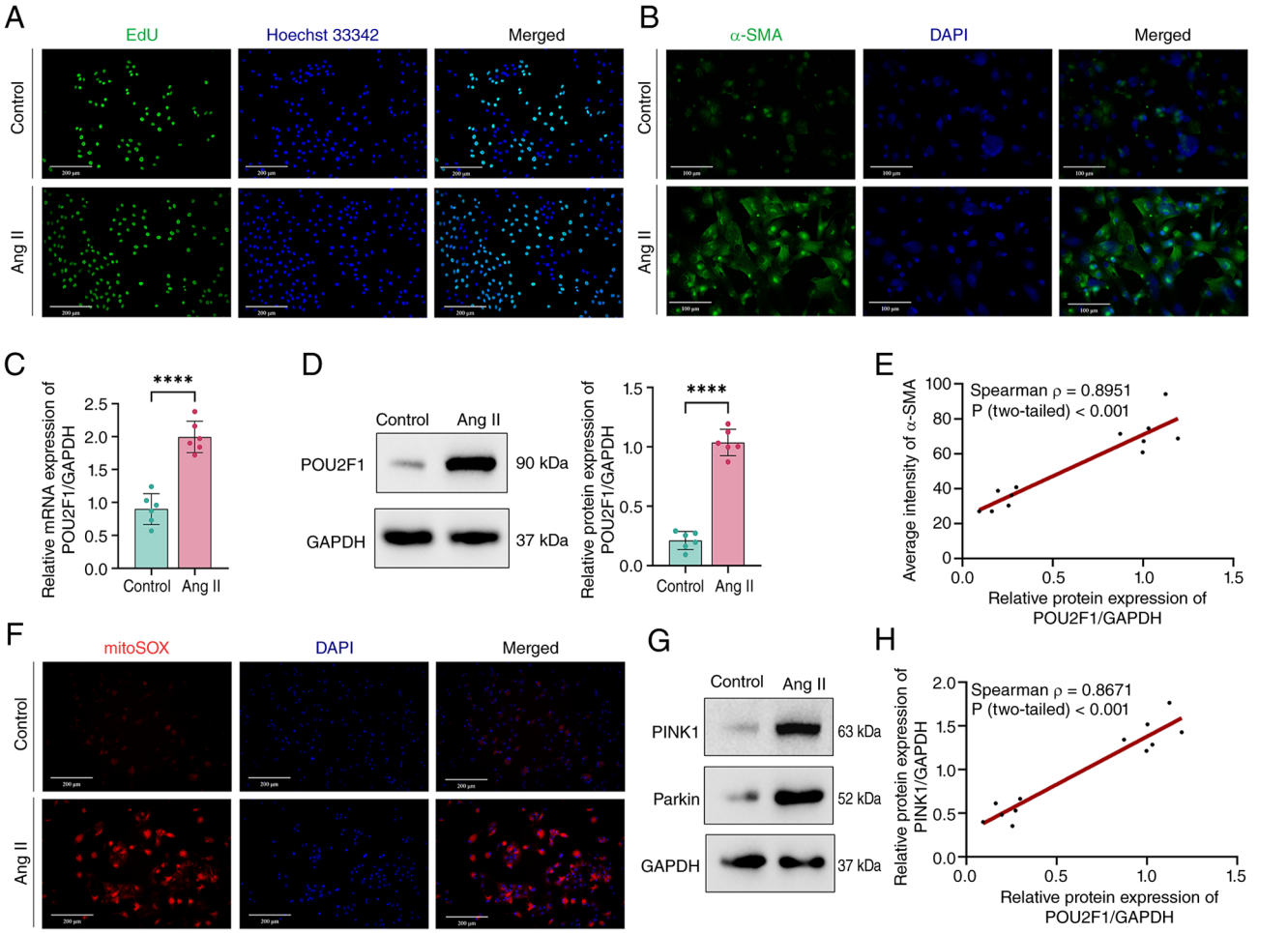

Figure 2. POU2F1 upregulation and mitochondrial damage in Ang II-induced CFs. (A) CF proliferation was assessed using an EdU assay (scale bar, 200 μm). (B) Representative immunofluorescence staining of α-SMA in CFs (scale bar, 100 μm). (C) mRNA levels of POU2F1 in CFs were detected by reverse transcription-quantitative PCR (n=6). (D) Protein levels of POU2F1 in CFs were detected by western blotting (n=6). (E) α-SMA fluorescence intensity was positively correlated with the protein expression levels of POU2F1 in CFs (Spearman correlation, n=12). (F) MitoSOX staining showing levels of mitochondrial superoxide in CFs (scale bar, 200 μm). (G) Protein levels of PINK1 and Parkin in CFs were detected by western blotting (n=6). (H) Protein expression levels of PINK1 were positively correlated with POU2F1 expression in CFs (Spearman correlation, n=12). Data are presented as the mean ± SD. (C and D) Unpaired two-tailed Student's t-test were used for statistical analysis. ****P<0.0001. α-SMA, α-smooth muscle actin; Ang II, angiotensin II; CF, cardiac fibroblast; PINK1, PTEN-induced kinase 1; POU2F1, POU domain class 2 transcription factor 1.

POU2F1 knockdown, thus indicating that Ang II-induced fibrotic remodeling was attenuated (Fig. 3I).

PINK1 knockdown reverses POU2F1 overexpression-induced myocardial fibrosis. The current study generated plasmids to induce POU2F1 overexpression and PINK1 knockdown, with the aim of further investigating the role of the POU2F1/PINK1 signaling pathway in myocardial fibrosis. The overexpression efficiency of POU2F1 and knockdown efficiency of PINK1 were confirmed by RT-qPCR analysis in CFs (Fig. S3B). A significant increase in both CF proliferation (Fig. 4A and C) and α-SMA expression (Fig. 4B and D) was observed following POU2F1 overexpression. Furthermore, consistent with the pro-fibrotic phenotype, elevated expression levels of collagen I and α-SMA proteins were detected in response to POU2F1 overexpression (Fig. 4E and F). Notably, this pro-fibrotic effect was attenuated by PINK1 knockdown. These findings highlight the key role of PINK1 in the regulation of myocardial fibrosis.

PINK1 knockdown reduces mitophagy and myocardial fibrosis independent of POU2F1 expression in Ang II-induced CFs. To investigate the potential interplay between POU2F1 and PINK1, gene-specific knockdown experiments were performed in CFs. POU2F1 knockdown significantly reduced PINK1 expression, whereas PINK1 knockdown did not alter POU2F1 protein levels in Ang II-induced CFs (Fig. 5A and B), suggesting a unidirectional regulatory role of POU2F1 over PINK1. These findings indicated that POU2F1 does not directly interact with PINK1 but may function as an upstream transcriptional regulator of PINK1 expression. Given the central role of PINK1 in mitophagy, the current study next assessed the effects of PINK1 knockdown on the mitophagy pathway. In Ang II-induced CFs, knockdown of PINK1 significantly decreased the expression levels of key mitophagy-related proteins, including PINK1, Parkin and LC3B, while inducing the accumulation of P62, collectively indicating suppression of mitophagy (Fig. 5C). Furthermore, PINK1 knockdown resulted in an attenuation of collagen I and α-SMA levels (Fig. 5D). Collectively, these results demonstrated that PINK1-mediated

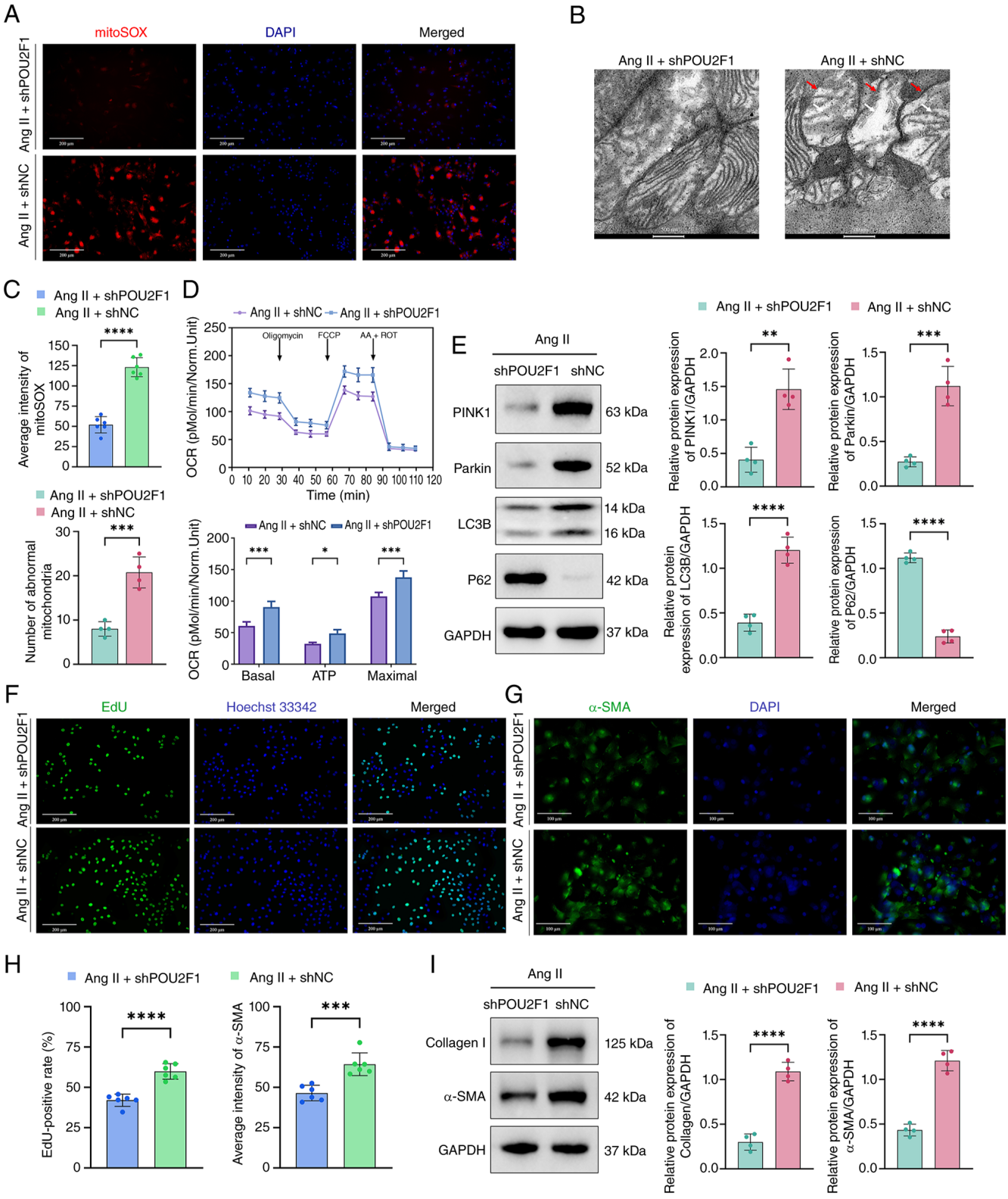

Figure 3. POU2F1 knockdown reduces PINK1-mediated mitophagy and mitochondrial dysfunction in Ang II-induced CFs. (A) MitoSOX staining showing levels of mitochondrial superoxide in Ang II-induced CFs infected with shPOU2F1 or shNC (scale bar, 200 μm). (B) Transmission electron microscopy was used to observe mitochondrial structure (scale bar, 500 nm). White arrows indicate cristae disorganization; red arrows indicate damaged mitochondria. (C) Quantification of MitoSOX fluorescence intensity was performed (n=6). Quantification of abnormal mitochondria was performed using low-magnification TEM images (x5,300 magnification; n=4). (D) Seahorse assay profile of OCRs in CFs following treatment with oligomycin, FCCP and AA + ROT. Quantitative analysis of mitochondrial function parameters (basal respiration, maximal respiration and ATP production) is shown in the bar charts (n=3). (E) Western blotting was utilized to determine the protein expression levels of PINK1, Parkin, LC3B and P62 (n=4). (F) CF proliferation was assessed using an EdU assay (scale bar, 200 μm). (G) Representative immunofluorescence images of α-SMA (scale bar, 100 μm). (H) Quantification of EdU-positive cells and α-SMA expression (n=6). (I) Western blotting was utilized to determine the protein expression levels of collagen I and α-SMA (n=4). Data are presented as the mean ± SD. (C-E, H and I) Unpaired two-tailed Student's t-test was used for statistical analysis. *P<0.05; **P<0.01; ***P<0.001; ****P<0.0001. α-SMA, α-smooth muscle actin; AA, antimycin A; Ang II, angiotensin II; CF, cardiac fibroblast; FCCP, carbonyl cyanide-4-trifluoromethoxy phenylhydrazone; NC, negative control; OCR, oxygen consumption rate; PINK1, PTEN-induced kinase 1; POU2F1, POU domain class 2 transcription factor 1; ROT, rotenone; sh, short hairpin.

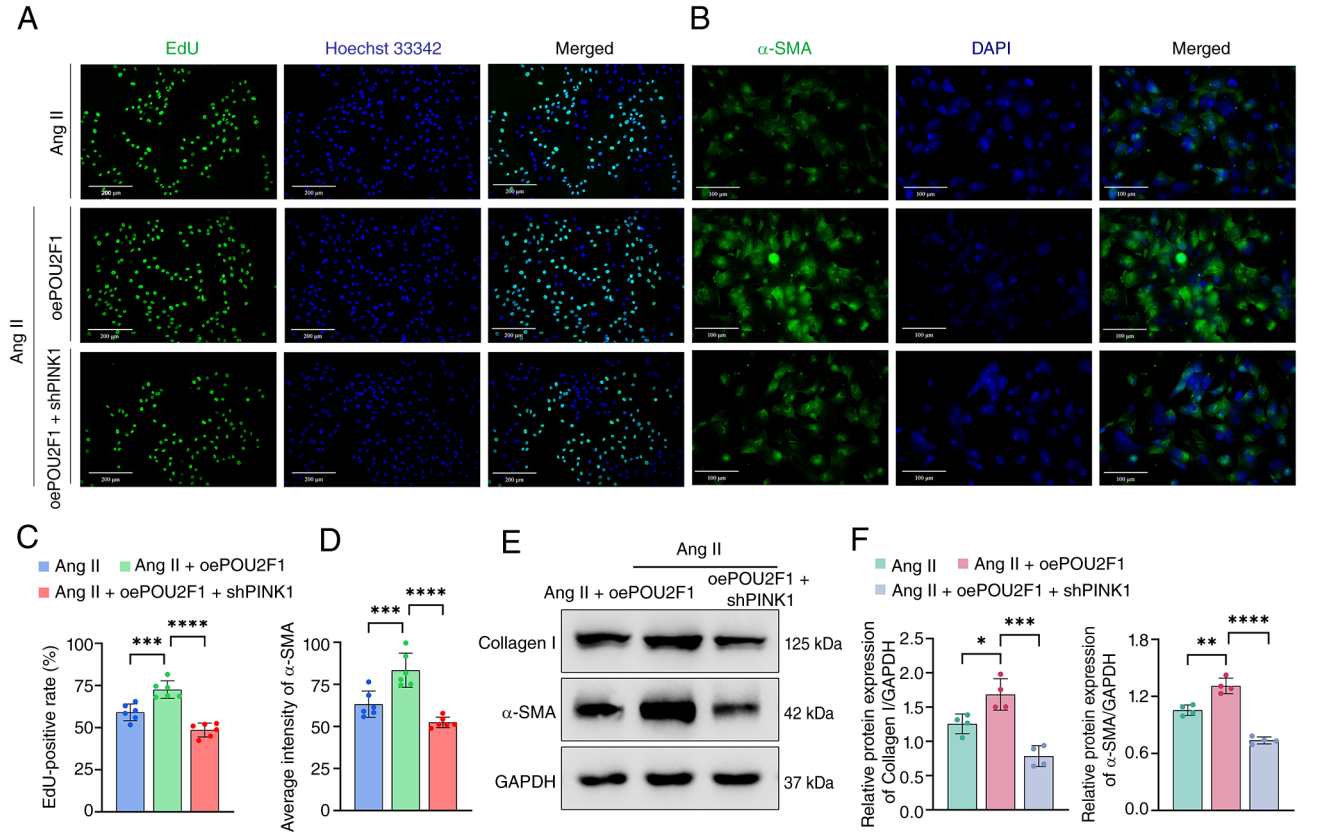

Figure 4. PINK1 knockdown reverses oePOU2F1-induced myocardial fibrosis. (A) Proliferation of Ang II-induced cardiac fibroblasts was assessed following different interventions using an EdU assay (scale bar, 200 μm). (B) Representative immunofluorescence images of α-SMA (scale bar, 100 μm). (C) Rate of EdU-positive cells was quantified (n=6). (D) Quantification of the average intensity of α-SMA fluorescence (n=6). (E) Western blotting was utilized to determine the protein expression levels of collagen I and α-SMA. (F) Semi-quantification of collagen I and α-SMA protein expression (n=4). *P<0.05; **P<0.01; ***P<0.001; ****P<0.0001. α-SMA, α-smooth muscle actin; Ang II, angiotensin II; oe, overexpression; PINK1, PTEN-induced kinase 1; POU2F1, POU domain class 2 transcription factor 1; sh, short hairpin.

mitophagy critically contributes to Ang II-induced myocardial fibrosis, and POU2F1 likely exerts profibrotic effects by modulating PINK1 transcription.

POU2F1 directly binds to the PINK1 gene promoter to enhance PINK1 transcription. Bioinformatics analysis was next performed to elucidate POU2F1-mediated transcriptional regulation of PINK1. The rat PINK1 promoter sequence (-2,000 bp) was retrieved from NCBI, with Jaspar software predicting a POU2F1-binding motif; POU2F1 was identified as a transcription factor binding to the PINK1 promoter at the specific motif TATTTAAAT (Fig. 6A). The specific binding of POU2F1 was validated using a series of complementary experiments. First, ChIP assays using an anti-POU2F1 antibody demonstrated significant enrichment of the PINK1 promoter region compared with the IgG control, confirming the binding of POU2F1 to the PINK1 promoter (Fig. 6B). To characterize the specificity of this interaction, EMSA was performed. POU2F1 protein bound specifically to a fluorescently labeled probe (lane 3) containing the consensus wild-type sequence (TATTTAAAT). Notably, this binding was competitively inhibited by an excess of unlabeled wild-type probes (lane 2), but was unaffected by a mutated probe (lane 4), underscoring the sequence-specific nature of the binding (Fig. 6D). Finally, a dual-luciferase reporter assay was conducted to determine the functional relevance of this binding; this confirmed that the direct binding of POU2F1 to the PINK1 promoter robustly enhanced its transcriptional activity (Fig. 6C).

POU2F1 overexpression was utilized to validate its regulation of PINK1. Western blotting and RT-qPCR confirmed that the mRNA and protein expression levels of PINK1 were enhanced following POU2F1 overexpression (Fig. 6E and F). Collectively, these findings confirmed that POU2F1 binds to specific motifs in the PINK1 promoter and drive its transcription.

POU2F1 knockdown reduces PINK1-mediated mitochondrial dysfunction and cardiac fibrosis in SHRs. To clarify the effects of POU2F1 on hypertension-induced cardiac fibrosis in SHRs, AAV9 vectors encoding shPOU2F1 or shNC were constructed and injected into 14-week-old SHRs via the tail vein. After 4 weeks, AAV9-shPOU2F1 achieved efficient myocardial transduction, significantly reducing POU2F1 expression (Fig. 7A). Furthermore, compared with the AAV9-shNC group, POU2F1 knockdown in SHRs significantly decreased myocardial PINK1 and Parkin expression (Fig. 7B). In AAV9-shPOU2F1-induced SHRs, TEM and Seahorse metabolic assays confirmed that mitochondrial damage was alleviated and mitochondrial respiratory function was improved (Fig. 7C and D). The fibrotic area of the cardiac tissues was also markedly decreased (Fig. 7E), with a concomitant downregulation of collagen I and α-SMA

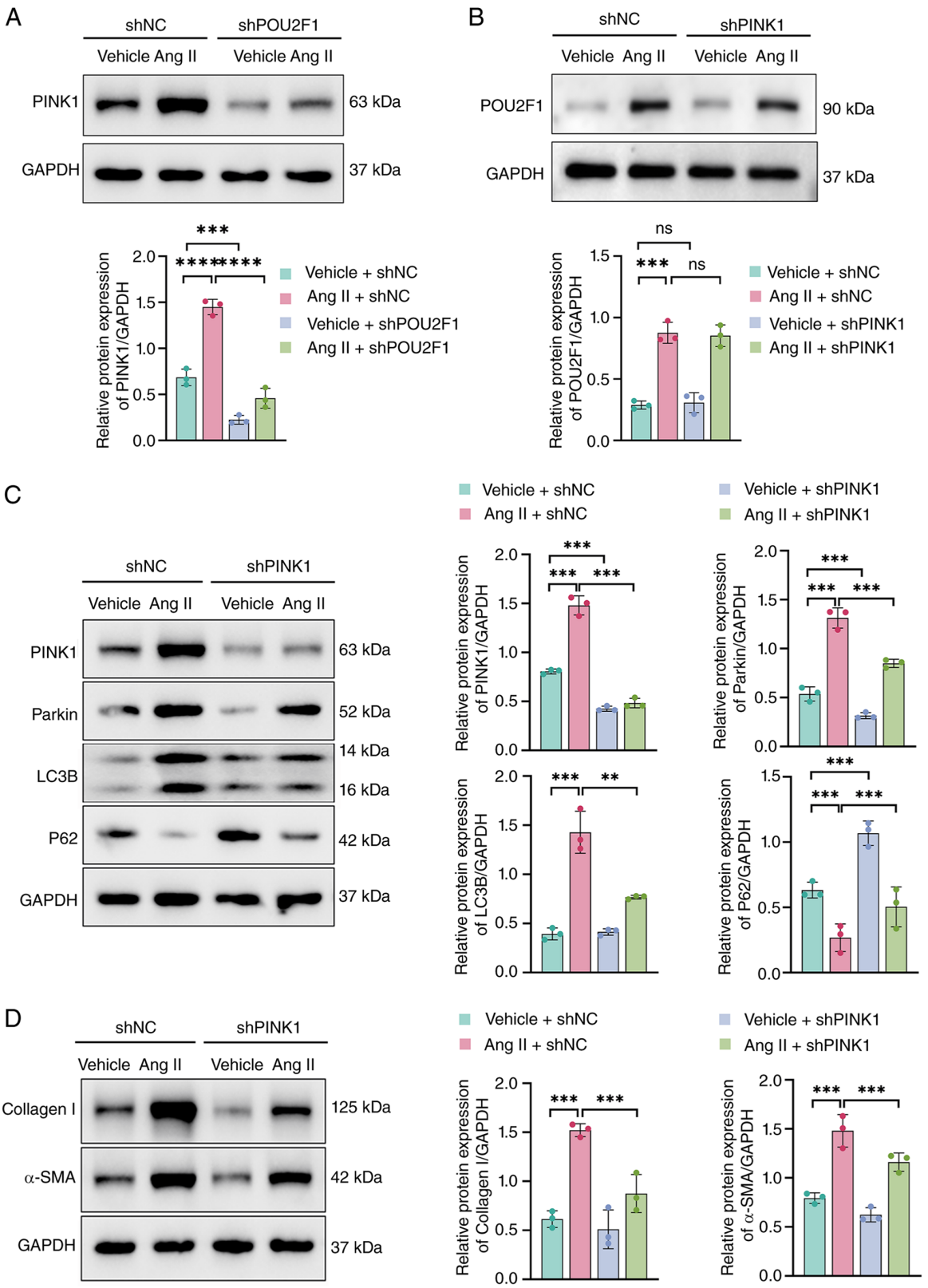

Figure 5. PINK1 knockdown reduces mitophagy and myocardial fibrosis independent of POU2F1 expression in Ang II-induced cardiac fibroblasts. Western blotting was utilized to determine the protein expression levels of (A) PINK1 and (B) POU2F1 (n=3). Expression levels of (C) PINK1, Parkin, LC3B and P62, as well as (D) collagen I and α-SMA were determined using western blotting (n=3). **P<0.01; ***P<0.001; ****P<0.0001. α-SMA, α-smooth muscle actin; Ang II, angiotensin II; ns, not significant; NC, negative control; PINK1, PTEN-induced kinase 1; POU2F1, POU domain class 2 transcription factor 1; sh, short hairpin.

protein expression (Fig. 7F). Echocardiography demonstrated an improvement in cardiac structure compared with in the SHR + AAV9-shNC group, with reduced interventricular septal thickness (IVSD and IVSS) and posterior wall thickness (LVPWD and LVPWS), and increased left ventricular internal dimensions (LVIDD and LVIDS) (Fig. 7G and H). Overall,

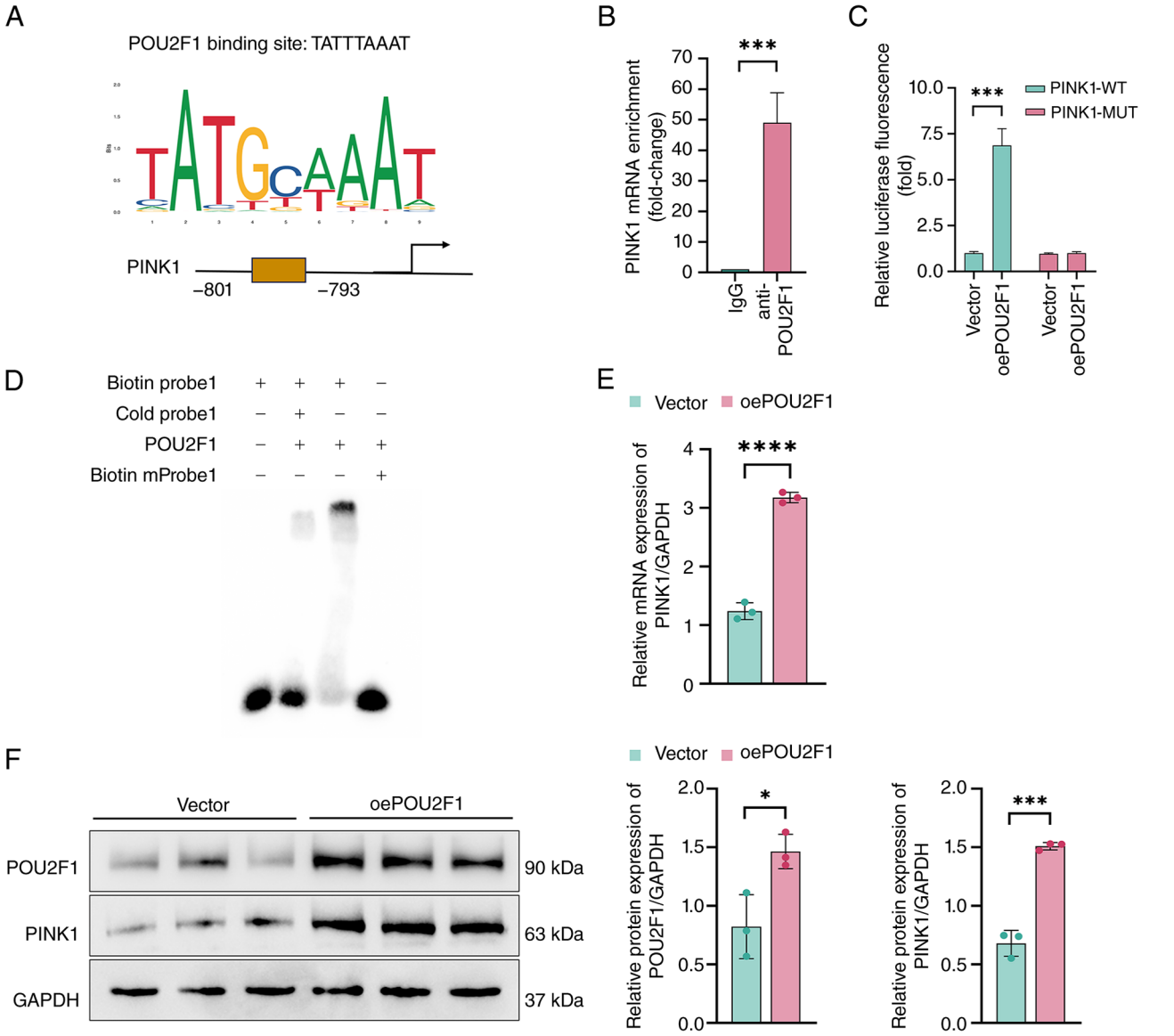

Figure 6. POU2F1 directly binds the PINK1 gene promoter to enhance PINK1 transcription. (A) Schematic of the binding site between POU2F1 and the PINK1 promoter region. (B) Chromatin immunoprecipitation-qPCR was performed to determine the binding of POU2F1 to the promoter sequence of PINK1 (n=3). IgG was applied as a negative control. (C) 293T cells were transfected with WT or MUT PINK1 plasmids and then transfected with vector or oePOU2F1 plasmid. A dual-luciferase reporter assay was performed (n=3). (D) Electrophoretic mobility shift assay was employed to analyze the interaction between POU2F1 and the PINK1 promoter fragment. (E) Following transfection with oePOU2F1 or empty vector, the mRNA levels of PINK1 in cardiac fibroblasts were quantified by reverse transcription-qPCR (n=3). (F) Protein levels of POU2F1 and PINK1 were detected by western blotting (n=3). Data are presented as the mean ± SD. (B, C, E and F) Unpaired two-tailed Student's t-test was used for statistical analysis. *P<0.05; ***P<0.001; ****P<0.0001. MUT, mutant; oe, overexpression; PINK1, PTEN-induced kinase 1; POU2F1, POU domain class 2 transcription factor 1; qPCR, quantitative PCR; WT, wild-type.

these findings demonstrated that inhibiting the expression of POU2F1 may suppress PINK1-mediated mitochondrial dysfunction and reduce cardiac fibrosis in SHRs.

Discussion

Hypertension is known to induce mitochondrial damage, increase collagen deposition and drive myocardial fibrosis. While PINK1-mediated mitophagy is a well-characterized pathway, its upstream regulatory mechanisms in hypertension-induced cardiac fibrosis remain incompletely understood. The present study provided the following key insights: i) POU2F1 acts as a critical regulator, which is significantly elevated in both SHRs and Ang II-induced CFs, exacerbating hypertension-induced cardiac fibrosis. ii) POU2F1 is associated with enhanced PINK1/Parkin-mediated mitophagy-related signaling, accompanied by disrupted mitochondrial homeostasis. iii) POU2F1, as a transcription factor, directly binds to the PINK1 promoter to enhance PINK1 transcription and expression. These findings indicated that POU2F1-regulated mitochondrial homeostasis is a potential target for hypertensive cardiac remodeling therapies (Fig. 8).

Hypertension represents a major risk factor for cardiovascular diseases, as it not only elevates cardiac afterload but also triggers progressive pathological cardiac remodeling, ultimately leading to heart failure (43-45). In the damaged heart, CFs express excessive levels of cytokines, including transforming growth factor-β, IL-1β) and interleukin-6 (IL-6),

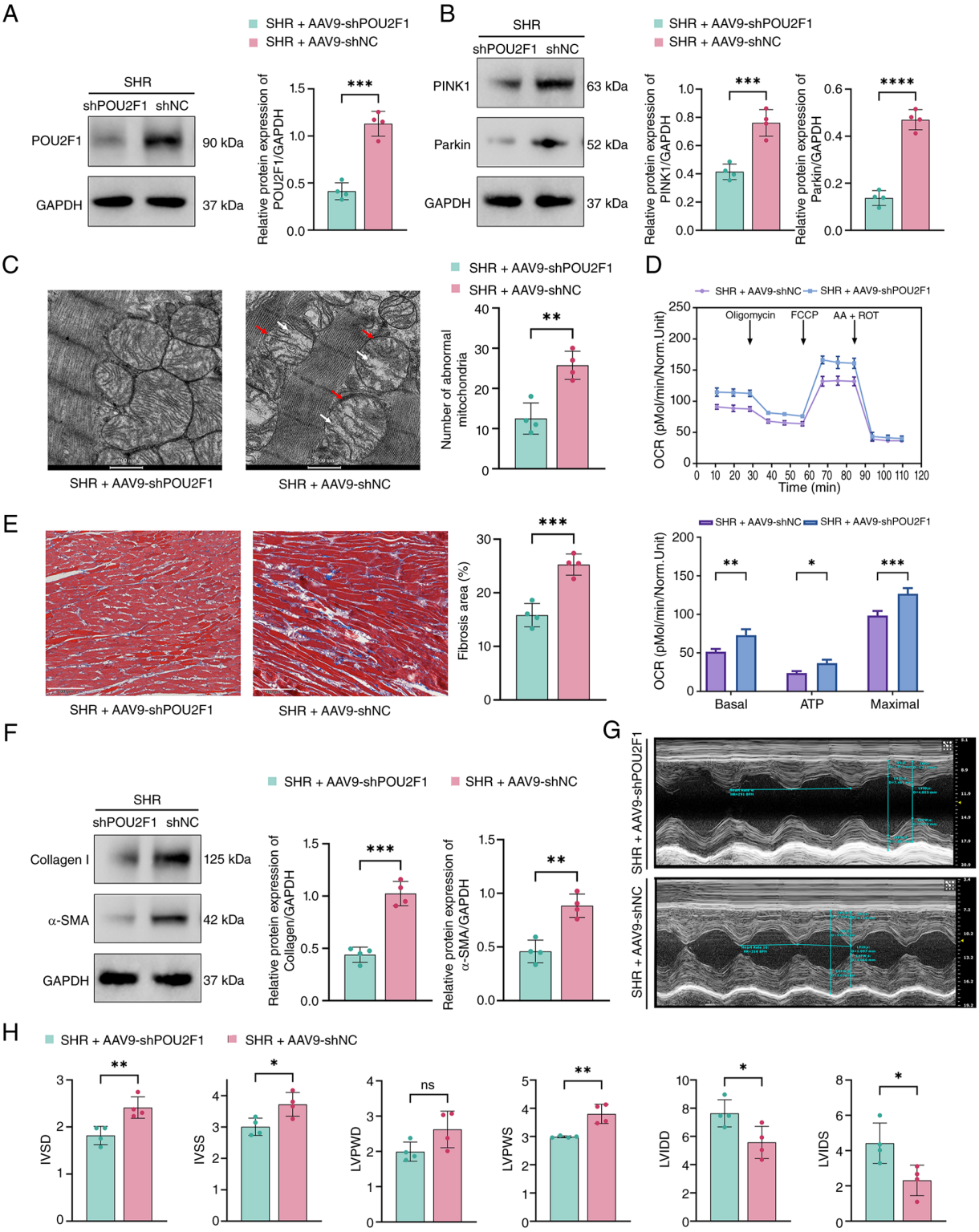

Figure 7. POU2F1 knockdown reduces PINK1-mediated mitochondrial dysfunction and cardiac fibrosis in SHRs. Western blot analysis of (A) POU2F1, and (B) PINK1 and Parkin in SHRs infected with AAV9-shPOU2F1 or AAV9-shNC (n=4). (C) Transmission electron microscopy was used to observe the mitochondrial structure in cardiac tissue from SHRs infected with AAV9-shPOU2F1 or AAV9-shNC (scale bar, 500 nm). White arrows indicate cristae disorganization; red arrows indicate damaged mitochondria. (D) Seahorse assay profile of OCRs in CFs following treatment with oligomycin, FCCP and AA + ROT. Quantitative analysis of mitochondrial function parameters (basal respiration, maximal respiration and ATP production) is shown in the bar charts (n=3). (E) Interstitial myocardial fibrosis (blue) assessed via Masson's trichrome staining (scale bar, 100 μm; n=4). (F) Western blot analysis of collagen I and α-SMA protein expression in two groups (n=4). (G) Representative echocardiographic images of SHRs following different interventions. (H) Echocardiographic parameters, including IVSD, IVSS, LVPWD, LVPWS, LVIDD and LVIDS, were measured in the two groups (n=4). Data are presented as the mean ± SD. (A-F and H) Unpaired two-tailed Student's t-test was used for statistical analysis. ns, no significance; *P<0.05; **P<0.01; ***P<0.001; ****P<0.0001. α-SMA, α-smooth muscle actin; AA, antimycin A; AAV9, adeno-associated virus serotype 9; FCCP, carbonyl cyanide-4-trifluoromethoxy phenylhydrazone; IVSD, interventricular septal diastolic thickness; IVSS, interventricular septal systolic thickness; LVIDD, left ventricular end-diastolic diameter; LVIDS, left ventricular end-systolic diameter; LVPWD, left ventricular posterior wall diastolic thickness; LVPWS, left ventricular posterior wall systolic thickness; NC, negative control; OCR, oxygen consumption rate; PINK1, PTEN-induced kinase 1; POU2F1, POU domain class 2 transcription factor 1; ROT, rotenone; sh, short hairpin; SHR, spontaneously hypertensive rat.

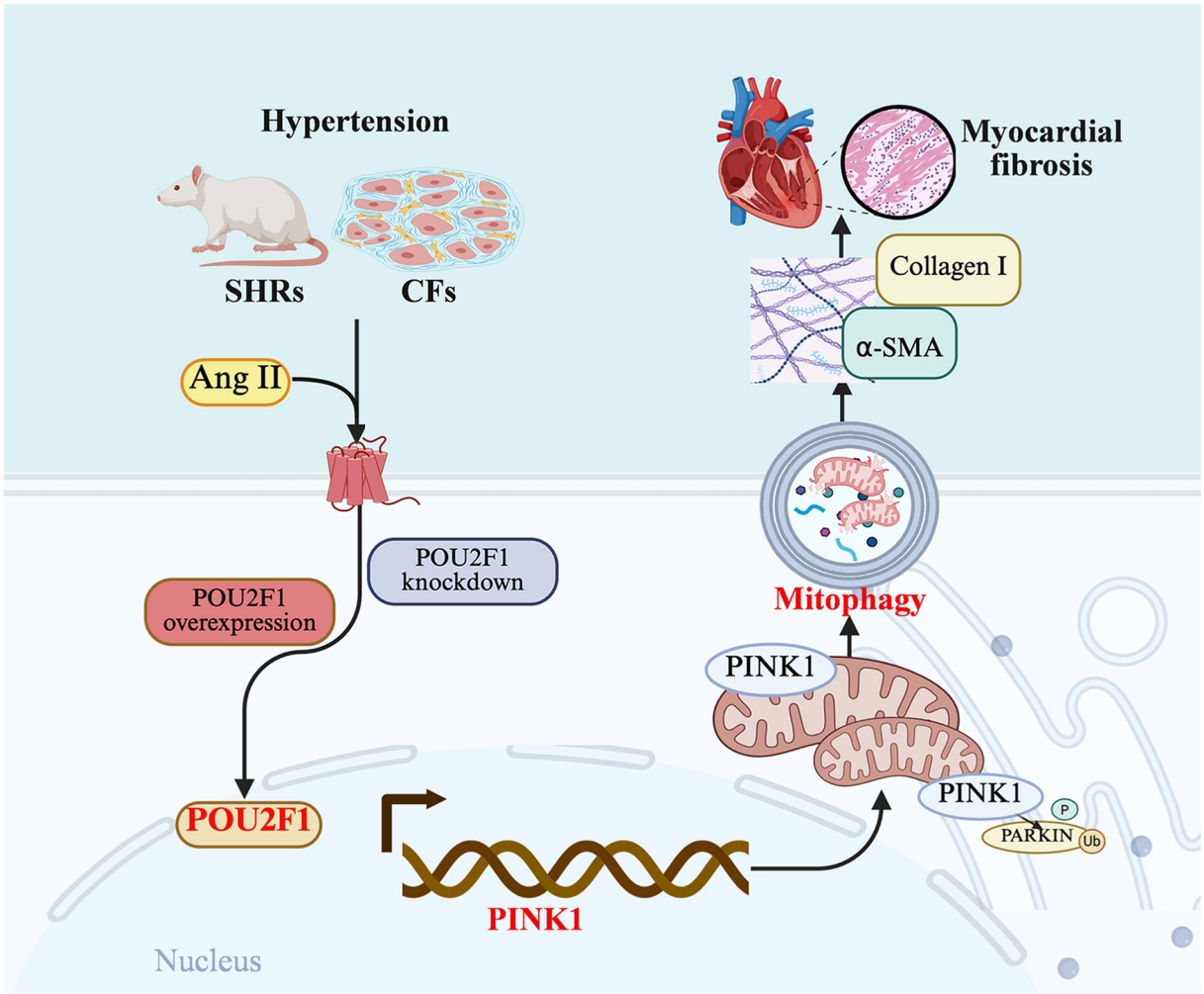

Figure 8. POU2F1 promotes hypertensive cardiac fibrosis by regulating mitochondrial homeostasis through PINK1/Parkin-dependent mitophagy. α-SMA, α-smooth muscle actin; Ang II, angiotensin II; CF, cardiac fibroblast; PINK1, PTEN-induced kinase 1; POU2F1, POU domain class 2 transcription factor 1.

leading to the enhanced proliferation of CFs, myofibroblast activation and excessive secretion of ECM components (46). The present study revealed that POU2F1 expression exhibited a positive correlation with the severity of myocardial fibrosis in both SHRs and Ang II-induced CFs. Knockdown of POU2F1 *in vitro* suppressed the expression of α-SMA and collagen I, whereas its overexpression conversely promoted their expression. Moreover, knockdown of POU2F1 in SHRs attenuated cardiac fibrosis and improved cardiac function, which further confirms the critical role of POU2F1 in hypertension-induced cardiac fibrosis. These results extend the findings of previous studies on transcriptional regulation in cardiac fibrosis, which have primarily focused on factors such as TGF-β/Smad, NF-κB and other transcription factors, by introducing POU2F1 as a novel participant in this network (47-49).

Transcription factors bind to specific cis-acting elements in the promoter or enhancer regions of target genes, thereby activating or repressing transcriptional initiation and modulating the spatiotemporal expression of downstream genes (50,51). Previous studies have demonstrated that POU2F1 can directly bind to the promoters of target genes such as aldolase A and lactate dehydrogenase A to promote the proliferation of tumor cells (52,53). However, its function in cardiac fibrosis remains incompletely elucidated. A key insight from the present study is the direct transcriptional regulation of PINK1 by POU2F1. A strong positive correlation was observed between POU2F1 and PINK1 expression in SHRs and Ang II-induced CFs. Notably, POU2F1 overexpression markedly promoted PINK1 expression and myocardial fibrosis, and this effect was abrogated by PINK1 knockdown, indicating that the pro-fibrotic effects of POU2F1 are PINK1-dependent. To demonstrate this direct regulatory relationship, the binding sites for POU2F1 were predicted within the PINK1 promoter. Using EMSA and a dual-luciferase reporter assay, it was established that POU2F1 can bind directly to the PINK1 promoter, an interaction that may enhance both PINK1 transcription and its protein expression. This is consistent with evidence that transcription factors coordinate the fibrotic response by regulating gene expression in CFs (54,55). The present study therefore reveals a novel transcriptional regulatory mechanism linked to mitophagy modulation.

PINK1/Parkin-mediated mitophagy is crucial for maintaining cell homeostasis, and is important in the prevention and treatment of cardiovascular diseases (56,57). PINK1, a serine/threonine kinase located on depolarized mitochondria, is rapidly degraded upon entering the

mitochondria under physiological conditions (58). However, when PINK1 is upregulated, it accumulates on depolarized mitochondria and self-activates, recruiting Parkin to ubiquitinate mitochondrial substrates (59). These proteins bind to autophagosomes and are ultimately transported to lysosomes, completing the mitophagy process. Mitophagy has emerged as a double-edged sword in cardiac biology, with moderate activation promoting cell survival under stress, whereas excessive or aberrant mitophagy can contribute to tissue damage (60-62). In the present study, elevated expression of PINK1, Parkin and LC3B in both SHRs and Ang II-induced CFs confirmed the occurrence of excessive mitophagy. Knockdown of PINK1 in Ang II-induced CFs downregulated mitophagy-associated proteins and attenuated myocardial fibrosis. Furthermore, both *in vivo* and *in vitro*, knockdown of POU2F1 suppressed PINK1 transcription and expression, which similarly led to the inhibition of mitophagy. A limitation of the present study is the lack of direct TEM evidence of mitochondria-containing autophagosomes. Given the transient nature of mitophagy and the limited sampling scope of ultrastructural imaging, further assessment of mitophagic flux is warranted. Nevertheless, mitochondrial structural damage, impaired respiratory function, and increased PINK1 and Parkin expression suggest dysregulation of the PINK1/Parkin-mediated mitophagy pathway.

Excessive mitophagy disrupts mitochondrial homeostasis, thereby contributing to the pathogenesis of fibrotic diseases (63-65). Activation of sirtuin 3 has been shown to suppress mitochondrial oxidative stress and activate the AMPK/Parkin axis, thereby mitigating mitochondrial damage and improving cardiac function (66). The hypoxia-inducible factor 1α/BCL2-interacting protein 3 signaling pathway is involved in mitophagy and serves a protective role in renal fibrosis (67). Furthermore, high temperature requirement protein A2 expression regulates mitochondrial DNA damage and mitochondrial homeostasis in hepatocytes during liver fibrogenesis (68). To the best of our knowledge, the present study is the first to elucidate the regulation of mitochondrial homeostasis by POU2F1. POU2F1 was knocked down in SHRs and Ang II-induced CFs, and it was observed that the mitophagy-related proteins PINK1, Parkin and LC3B were downregulated, accompanied by alleviated mitochondrial structural damage, improved mitochondrial respiratory function and a reduced degree of myocardial fibrosis. This result confirmed that POU2F1 may promote hypertensive cardiac fibrosis by regulating mitochondrial homeostasis.

In summary, the present study established POU2F1 as a key upstream regulator that is significantly upregulated in hypertensive models. POU2F1 directly bind to the PINK1 promoter to potentiate its transcription, thereby enhancing PINK1/Parkin-associated mitophagy-related signaling and driving cardiac fibrotic remodeling. This finding highlights POU2F1 as a promising therapeutic target; therefore, modulating its expression to restore mitochondrial homeostasis may halt fibrotic remodeling.

Acknowledgements

Not applicable.

Funding

The authors declare that financial support was received for the research and/or publication of this article; this work was supported by grants from the National Natural Science Foundation of China (grant nos. 82174130 and 82274262), the Shanghai Science and Technology Innovation Program for Cultivation of Lightening Stars (Yangfan Project) (grant no. 23YF1448400), the Shanghai 'Rising Stars of Medical Talents' Youth Development Program (Youth Medical Talents-Specialist Program) (grant no. RY411.19.01.14), the Shanghai Magnolia Talent Plan Pujiang Project (grant no. 24PJD113) and the Shanghai Municipal Health Commission Traditional Chinese Medicine Research Project (grant no. 2022QN031).

Availability of data and materials

The RNA-seq data generated in the present study may be found in the OMIX (China National Center for Bioinformation) database under accession number OMIX018255 or at the following URL: https://ngdc.cncb.ac.cn/omix/release/OMIX018255. The other data generated in the present study may be requested from the corresponding author.

Authors' contributions

DYF and MZW designed the experiments. YBM, XZC and ZXL performed the experiments and drafted the manuscript. YLM and MTG helped with the experiments. CLH, YFL and BL analyzed the data. All authors read and approved the final manuscript. YBM and XZC confirm the authenticity of all the raw data.

Ethics approval and consent to participate

The present study was performed at Yueyang Hospital of Integrated Traditional Chinese and Western Medicine, and the animal study was approved by the Institutional Animal Care and Use Committee of Yueyang Hospital of Integrated Traditional Chinese and Western Medicine (approval no. YYLAC-2023-182-1) following the National Institutes of Health guidelines.

Patient consent for publication

Not applicable.

Competing interests

The authors declare that they have no competing interests.

References

1. NCD Risk Factor Collaboration (NCD-RisC): Worldwide trends in hypertension prevalence and progress in treatment and control from 1990 to 2019: A pooled analysis of 1201 population-representative studies with 104 million participants. Lancet 398: 957-980, 2021.
2. Shinde AV, Humeres C and Frangogiannis NG: The role of α-smooth muscle actin in fibroblast-mediated matrix contraction and remodeling. Biochim Biophys Acta Mol Basis Dis 1863: 298-309, 2017.

3. Querejeta R, López B, González A, Sánchez E, Larman M, Martínez Ubago JL and Díez J: Increased collagen type I synthesis in patients with heart failure of hypertensive origin: relation to myocardial fibrosis. Circulation 110: 1263-1268, 2004.
4. Liu T, Song D, Dong J, Zhu P, Liu J, Liu W, Ma X, Zhao L and Ling S: Current understanding of the pathophysiology of myocardial fibrosis and its quantitative assessment in heart failure. Front Physiol 8: 238, 2017.
5. Gibb AA, Lazaropoulos MP and Elrod JW: Myofibroblasts and fibrosis: Mitochondrial and metabolic control of cellular differentiation. Circ Res 127: 427-447, 2020.
6. Lin LC, Tu B, Song K, Liu ZY, Sun H, Zhou Y, Sha JM, Yang JJ, Zhang Y, Zhao JY and Tao H: Mitochondrial quality control in cardiac fibrosis: Epigenetic mechanisms and therapeutic strategies. Metabolism 145: 155626, 2023.
7. Li B, Liu F, Chen X, Chen T, Zhang J, Liu Y, Yao Y, Hu W, Zhang M, Wang B, *et al*: FARS2 deficiency causes cardiomyopathy by disrupting mitochondrial homeostasis and the mitochondrial quality control system. Circulation 149: 1268-1284, 2024.
8. Lin J, Chen X, Du Y, Li J, Guo T and Luo S: Mitophagy in cell death regulation: Insights into mechanisms and disease implications. Biomolecules 14: 1270, 2024.
9. Palikaras K, Lionaki E and Tavernarakis N: Mechanisms of mitophagy in cellular homeostasis, physiology and pathology. Nat Cell Biol 20: 1013-1022, 2018.
10. Nguyen TN, Padman BS and Lazarou M: Deciphering the molecular signals of PINK1/Parkin mitophagy. Trends Cell Biol 26: 733-744, 2016.
11. Hu J, Liu T, Fu F, Cui Z, Lai Q, Zhang Y, Yu B, Liu F, Kou J and Li F: Omentin1 ameliorates myocardial ischemia-induced heart failure via SIRT3/FOXO3a-dependent mitochondrial dynamical homeostasis and mitophagy. J Transl Med 20: 447, 2022.
12. Ren S, Wang Y, Zhang Y, Yan P, Xiao D, Zhao Y, Jia W, Ding L, Dong H, Wei C, *et al*: Paeoniflorin alleviates AngII-induced cardiac hypertrophy in H9c2 cells by regulating oxidative stress and Nrf2 signaling pathway. Biomed Pharmacother 165: 115253, 2023.
13. Li F, Fan X, Zhang Y, Zhang Y, Ma X, Kou J and Yu B: Inhibition of myosin IIA-actin interaction prevents ischemia/reperfusion induced cardiomyocytes apoptosis through modulating PINK1/Parkin pathway and mitochondrial fission. Int J Cardiol 271: 211-218, 2018.
14. Pan XC, Xiong YL, Hong JH, Liu Y, Cen YY, Liu T, Yang QF, Tao H, Li YN and Zhang HG: Cardiomyocytic FoxP3 is involved in Parkin-mediated mitophagy during cardiac remodeling and the regulatory role of triptolide. Theranostics 12: 2483-2501, 2022.
15. Zhang X, Li ZL, Crane JA, Jordan KL, Pawar AS, Textor SC, Lerman A and Lerman LO: Valsartan regulates myocardial autophagy and mitochondrial turnover in experimental hypertension. Hypertension 64: 87-93, 2014.
16. Ma Y, Zhou X, Gui M, Yao L, Li J, Chen X, Wang M, Lu B and Fu D: Mitophagy in hypertension-mediated organ damage. Front Cardiovasc Med 10: 1309863, 2024.
17. Ma Y, Li D, Zhou X, Chen X, Hou C, Li Y, Zhao Y, Gui M, Yao L, Li J, *et al*: METTL3-mediated m6A modification of FUNDC1/IP3R2 pathway facilitates cardiac hypertrophy in obesity hypertension. Life Sci 377: 123780, 2025.
18. Zhu HY, Cao GY, Wang SP, Chen Y, Liu GD, Gao YJ and Hu JP: POU2F1 promotes growth and metastasis of hepatocellular carcinoma through the FAT1 signaling pathway. Am J Cancer Res 7: 1665-1679, 2017.
19. Li F, Wang T and Huang Y: POU2F1 induces the immune escape in lung cancer by up-regulating PD-L1. Am J Transl Res 13: 672-683, 2021.
20. Li M, Wu J, Hu G, Song Y, Shen J, Xin J, Li Z, Liu W, Dong E, Xu M, *et al*: Pathological matrix stiffness promotes cardiac fibroblast differentiation through the POU2F1 signaling pathway. Sci China Life Sci 64: 242-254, 2021.
21. Yang W, Li Y, Bai J, You T, Yi K, Xie D, Zhang X and Xie X: A functional variant Rs492554 associated with congenital heart defects modulates SESN2 expression through POU2F1. Front Cell Dev Biol 9: 668474, 2021.
22. Feng N, Yu H, Wang Y, Zhang Y, Xiao H and Gao W: Exercise training attenuates angiotensin II-induced cardiac fibrosis by reducing POU2F1 expression. J Sport Health Sci 12: 464-476, 2023.
23. Liu N, Gong Z, Li Y, Xu Y, Guo Y, Chen W, Sun X, Yin X and Liu W: CTRP3 inhibits myocardial fibrosis through the P2X7R-NLRP3 inflammasome pathway in SHR rats. J Hypertens 42: 315-328, 2024.
24. Wang TJ, Lian GL, Lin X, Zhong HB, Xu CS, Wang HJ and Xie LD: Hypomethylation of Agtrap is associated with long-term inhibition of left ventricular hypertrophy in prehypertensive losartan-treated spontaneously hypertensive rats. Mol Med Rep 15: 839-846, 2017.
25. National Research Council (US) Committee for the Update of the Guide for the Care and Use of Laboratory Animals. Guide for the care and use of laboratory animals, 8th edition. National Academies Press, Washington, DC, 2011.
26. Tarbit E, Singh I, Peart JN, Bivol S and Rose Meyer RB: Increased release of serotonin from rat primary isolated adult cardiac myofibroblasts. Sci Rep 11: 20376, 2021.
27. Feng J, Li Y, Li Y, Yin Q, Li H, Li J, Zhou B, Meng J, Lian H, Wu M, *et al*: Versican promotes cardiomyocyte proliferation and cardiac repair. Circulation 149: 1004-1015, 2024.
28. Mao Q, Zhang X, Yang J, Kong Q, Cheng H, Yu W, Cao X, Li Y, Li C, Liu L and Ding Z: HSPA12A acts as a scaffolding protein to inhibit cardiac fibroblast activation and cardiac fibrosis. J Adv Res 67: 217-229, 2025.
29. Wu Y, Zhan S, Chen L, Sun M, Li M, Mou X, Zhang Z, Xu L and Xu Y: TNFSF14/LIGHT promotes cardiac fibrosis and atrial fibrillation vulnerability via PI3Kγ/SGK1 pathway-dependent M2 macrophage polarisation. J Transl Med 21: 544, 2023.
30. Guo J, Hang P, Yu J, Li W, Zhao X, Sun Y, Fan Z and Du Z: The association between RGS4 and choline in cardiac fibrosis. Cell Commun Signal 19: 46, 2021.
31. Vue Z, Garza-Lopez E, Neikirk K, Katti P, Vang L, Beasley H, Shao J, Marshall AG, Crabtree A, Murphy AC, *et al*: 3D reconstruction of murine mitochondria reveals changes in structure during aging linked to the MICOS complex. Aging Cell 22: e14009, 2023.
32. Rabinovich-Nikitin I, Rasouli M, Reitz CJ, Posen I, Margulets V, Dhingra R, Khatua TN, Thliveris JA, Martino TA and Kirshenbaum LA: Mitochondrial autophagy and cell survival is regulated by the circadian Clock gene in cardiac myocytes during ischemic stress. Autophagy 17: 3794-3812, 2021.
33. Hu R, Huang Y, Geng Y, Liu Z, Li F, Zhang Z, Ma W, Song K, Dong H, Song Y and Zhang M: Jiawei Buzhong Yiqi decoction ameliorates polycystic ovary syndrome via oocyte-granulosa cell communication. J Ethnopharmacol 323: 117654, 2024.
34. Stellato M, Dewenter M, Rudnik M, Hukara A, Özsoy Ç, Renoux F, Pachera E, Gantenbein F, Seebeck P, Uhtjaerv S, *et al*: The AP-1 transcription factor Fosl-2 drives cardiac fibrosis and arrhythmias under immunofibrotic conditions. Commun Biol 6: 161, 2023.
35. Convertini P, Santarsiero A, Todisco S, Gilio M, Palazzo D, Pappalardo I, Iacobazzi D, Frontuto M and Infantino V: ACLY as a modulator of liver cell functions and its role in metabolic dysfunction-associated steatohepatitis. J Transl Med 21: 568, 2023.
36. Zhang Y, Fan Y, Hu H, Zhang X, Wang Z, Wu Z, Wang L, Yu X, Song X, Xiang P, *et al*: ZHX2 emerges as a negative regulator of mitochondrial oxidative phosphorylation during acute liver injury. Nat Commun 14: 7527, 2023.
37. Liu M, Peng T, Hu L, Wang M, Guo D, Qi B, Ren G, Wang D, Li Y, Song L, *et al*: N-glycosylation-mediated CD147 accumulation induces cardiac fibrosis in the diabetic heart through ALK5 activation. Int J Biol Sci 19: 137-155, 2023.
38. Li Z, Hu O, Xu S, Lin C, Yu W, Ma D, Lu J and Liu P: The SIRT3-ATAD3A axis regulates MAM dynamics and mitochondrial calcium homeostasis in cardiac hypertrophy. Int J Biol Sci 20: 831-847, 2024.
39. Xie SY, Liu SQ, Zhang T, Shi WK, Xing Y, Fang WX, Zhang M, Chen MY, Xu SC, Fan MQ, *et al*: USP28 serves as a key suppressor of mitochondrial morphofunctional defects and cardiac dysfunction in the diabetic heart. Circulation 149: 684-706, 2024.
40. Berta DG, Kuisma H, Välimäki N, Räisänen M, Jäntti M, Pasanen A, Karhu A, Kaukomaa J, Taira A, Cajuso T, *et al*: Deficient H2A.Z deposition is associated with genesis of uterine leiomyoma. Nature 596: 398-403, 2021.
41. Zhang X, Huang DX, Xuan C, Li Y, Jiang Y, Wu X, Zhou W, Lei Y, Yang F, Ma H, *et al*: Aerobic exercise training attenuates ischemia-reperfusion injury in mice by decreasing the methylation level of METTL3-associated m6A RNA in cardiomyocytes. Life Sci 361: 123294, 2025.
42. Frangogiannis NG: Cardiac fibrosis. Cardiovasc Res 117: 1450-1488, 2021.
43. Chen YF, Qi RQ, Song JW, Wang SY, Dong ZJ, Chen YH, Liu Y, Zhou XY, Li J, Liu XY and Zhong JC: Sirtuin 7 ameliorates cuproptosis, myocardial remodeling and heart dysfunction in hypertension through the modulation of YAP/ATP7A signaling. Apoptosis 29: 2161-2182, 2024.

44. Yeo TM, Chin CWL, Seah CWA, Cheng LJ, Lin W, Dalakoti M, Foo R and Wang W: Global prevalence of myocardial fibrosis among individuals with cardiometabolic conditions: A systematic review and meta-analysis. Eur J Prev Cardiol 32: 1077-1091, 2025.
45. Iyer NR, Le TT, Kui MSL, Tang HC, Chin CT, Phua SK, Bryant JA, Pua CJ, Ang B, Toh DF, *et al*: Markers of focal and diffuse nonischemic myocardial fibrosis are associated with adverse cardiac remodeling and prognosis in patients with hypertension: the REMODEL study. Hypertension 79: 1804-1813, 2022.
46. Travers JG, Kamal FA, Robbins J, Yutzey KE and Blaxall BC: Cardiac fibrosis: The fibroblast awakens. Circ Res 118: 1021-1040, 2016.
47. Tuleta I, Hanna A, Humeres C, Aguilan JT, Sidoli S, Zhu F and Frangogiannis NG: Fibroblast-specific TGF-β signaling mediates cardiac dysfunction, fibrosis, and hypertrophy in obese diabetic mice. Cardiovasc Res 120: 2047-2063, 2024.
48. Umbarkar P, Ejantkar S, Tousif S and Lal H: Mechanisms of fibroblast activation and myocardial fibrosis: Lessons learned from FB-specific conditional mouse models. Cells 10: 2412, 2021.
49. Wang C, Luo H, Xu Y, Tao L, Chang C and Shen X: Salvianolic acid B-alleviated angiotensin II induces cardiac fibrosis by suppressing NF-κB pathway in vitro. Med Sci Monit 24: 7654-7664, 2018.
50. Lambert SA, Jolma A, Campitelli LF, Das PK, Yin Y, Albu M, Chen X, Taipale J, Hughes TR and Weirauch MT: The human transcription factors. Cell 172: 650-665, 2018.
51. Lee TI and Young RA: Transcriptional regulation and its misregulation in disease. Cell 152: 1237-1251, 2013.
52. Lin J, Xia L, Oyang L, Liang J, Tan S, Wu N, Yi P, Pan Q, Rao S, Han Y, *et al*: The POU2F1-ALDOA axis promotes the proliferation and chemoresistance of colon cancer cells by enhancing glycolysis and the pentose phosphate pathway activity. Oncogene 41: 1024-1039, 2022.
53. Wang H, Zhang F, Li L, Kang Z, Li J, Mao Y, Liu K, Song L and Shan S: POU2F1 facilitates the malignant phenotypes and aerobic glycolysis of pituitary adenoma by activating LDHA transcription. Brain Res 1866: 149870, 2025.
54. Hong JH and Zhang HG: Transcription factors involved in the development and prognosis of cardiac remodeling. Front Pharmacol 13: 828549, 2022.
55. Zhang Q, Wang L, Wang S, Cheng H, Xu L, Pei G, Wang Y, Fu C, Jiang Y, He C and Wei Q: Signaling pathways and targeted therapy for myocardial infarction. Signal Transduct Target Ther 7: 78, 2022.
56. Wu Y, Jiang T, Hua J, Xiong Z, Dai K, Chen H, Li L, Peng J, Peng X, Zheng Z and Xiong W: PINK1/Parkin-mediated mitophagy in cardiovascular disease: From pathogenesis to novel therapy. Int J Cardiol 361: 61-69, 2022.
57. D'Arcy MS: Mitophagy in health and disease. Molecular mechanisms, regulatory pathways, and therapeutic implications. Apoptosis 29: 1415-1428, 2024.
58. Narendra DP and Youle RJ: The role of PINK1-Parkin in mitochondrial quality control. Nat Cell Biol 26: 1639-1651, 2024.
59. Vizziello M, Borellini L, Franco G and Ardolino G: Disruption of mitochondrial homeostasis: The role of PINK1 in parkinson's disease. Cells 10: 3022, 2021.
60. Bravo-San Pedro JM, Kroemer G and Galluzzi L: Autophagy and mitophagy in cardiovascular disease. Circ Res 120: 1812-1824, 2017.
61. Li A, Gao M, Liu B, Qin Y, Chen L, Liu H, Wu H and Gong G: Mitochondrial autophagy: Molecular mechanisms and implications for cardiovascular disease. Cell Death Dis 13: 444, 2022.
62. Yang T, Yang Q, Lai Q, Zhao J, Nie L, Liu S, Yang J and Chu C: AP39 inhibits ferroptosis by inhibiting mitochondrial autophagy through the PINK1/parkin pathway to improve myocardial fibrosis with myocardial infarction. Biomed Pharmacother 165: 115195, 2023.
63. Lin D, Luo H, Dong B, He Z, Ma L, Wang Z, Wu X and Sui Q: FOXO3a induces myocardial fibrosis by upregulating mitophagy. Front Biosci (Landmark Ed) 29: 56, 2024.
64. Li Y, Zhao K, Hu Y, Yang F, Li P and Liu Y: MicroRNA-142-3p alleviated high salt-induced cardiac fibrosis via downregulating optineurin-mediated mitophagy. iScience 27: 109764, 2024.
65. Zhang YY, Zhou XT, Huang GZ, Liao WJ, Chen X and Ma YR: The pro-fibrotic role of autophagy in renal intrinsic cells: Mechanisms and therapeutic potential in chronic kidney disease. Front Cell Dev Biol 12: 1499457, 2024.
66. Peng F, Liao M, Jin W, Liu W, Li Z, Fan Z, Zou L, Chen S, Zhu L, Zhao Q, *et al*: 2-APQC, a small-molecule activator of Sirtuin-3 (SIRT3), alleviates myocardial hypertrophy and fibrosis by regulating mitochondrial homeostasis. Signal Transduct Target Ther 9: 133, 2024.
67. Li J, Lin Q, Shao X, Li S, Zhu X, Wu J, Mou S, Gu L, Wang Q, Zhang M, *et al*: HIF1α-BNIP3-mediated mitophagy protects against renal fibrosis by decreasing ROS and inhibiting activation of the NLRP3 inflammasome. Cell Death Dis 14: 200, 2023.
68. Hur W, Kang BY, Kim SM, Lee GW, Kim JH, Nam MK, Rhim H and Yoon SK: Serine protease HtrA2/Omi deficiency impairs mitochondrial homeostasis and promotes hepatic fibrogenesis via activation of hepatic stellate cells. Cells 8: 1119, 2019.